

Final Report to NASA
Multibeam Phased Array Antennas
 Program: High rate data delivery

PI: Prof. Zoya Popovic,
 Research Associates: Dr. Stefania Romisch, Dr. Sebastien Rondineau
 Department of Electrical and Computer Engineering
 University of Colorado at Boulder, Boulder, CO 80309

I. INTRODUCTION

In this study, a new architecture for Ka-band multi-beam arrays was developed and demonstrated experimentally. A working prototype was delivered to Dr. Richard Lee at NASA GRC.

The application relevant to the space program is communication between GEO satellites. The goal of the investigation was to demonstrate a new architecture that has the potential of reducing the cost as compared to standard expensive phased array technology. The following specifications were taken into account:

- Number of simultaneous T/R beams is $M=5$ to 6, although the delivered proof-of-principle prototype hardware has 4 beams, 2 for transmit and 2 for receive.
- Number of antenna array elements (N), i.e., antenna aperture size, is given by narrowest required beamwidth. For this study, a beamwidth of 5 to 10 degrees in both E and H planes is chosen
- Carrier frequency is in Ka-band, around 26GHz for up-link and 28GHz for down link, with a small (few percent) bandwidth
- Isolation between beams is an important parameter to be quantified
- Small continuous beam-steering is required within each beam for fine-tuning of about 5 degrees. This technology should also be low cost.
- Ultimately, it will be beneficial to add distributed gain to the antenna in both transmit and receive, and the array was designed with this in mind. Given additional funding, we would be able to design as a straightforward extension multibeam arrays with power gain.

The goals of this specific part of the project, as stated in the yearly statement of work in the original proposal are:

1. Investigate bounds on performance of multi-beam lens arrays in terms of beamwidths, volume (size), isolation between beams, number of simultaneous beams, etc.
2. Design a small-scale array to demonstrate the principle. The array will be designed for operation around 30GHz (Ka-band), with two 10-degree beamwidth beams.
3. Investigate most appropriate way to accomplish fine-tuning of the beam pointing within 5 degrees around the main beam pointing angle.

The basic proposed multi-beam architecture is shown in Fig.1 for the case of transmission. The antenna array is designed to be a spatially-fed amplifying lens. The front end array (labeled "radiating side antennas") determines the beamwidth as in standard antenna array theory. The multiple beams are obtained with multiple *spatial* feeds. The transmitters are placed along a

focal surface on the feed side of the array, and each position corresponds to a beam in a different direction. In Fig.1, three transmitters are shown as an example, corresponding to 3 simple beams. Any linear combination of the beams can also be performed to allow for beams of different widths, as will be described later. Note that the array is reciprocal (the amplifiers in the array are considered as bi-directional, as indicated by the symbol).

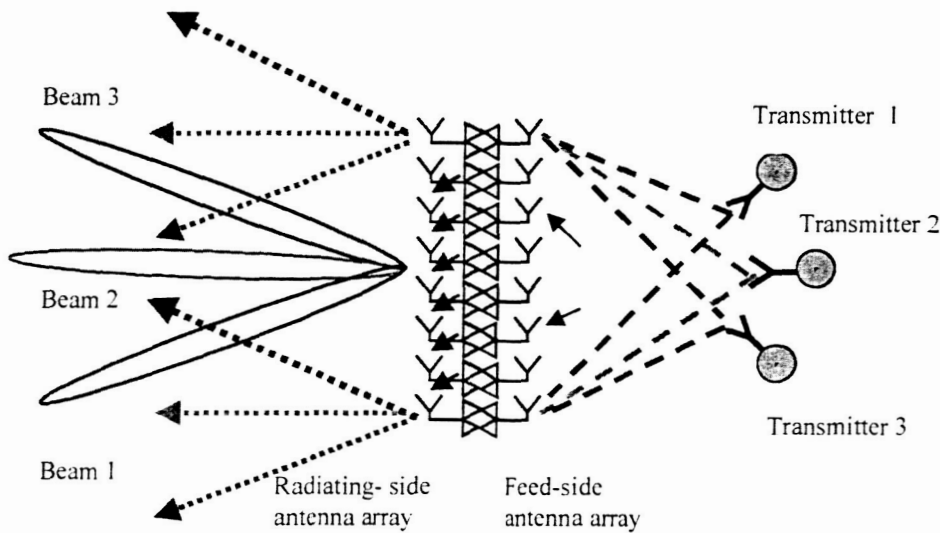


Figure 1. Sketch of transmit/receive lens array multibeam architecture with 3 beams given as an example. The array consists of radiating side elements and feed-side elements, connected through appropriate lensing delay lines and bidirectional amplifiers.

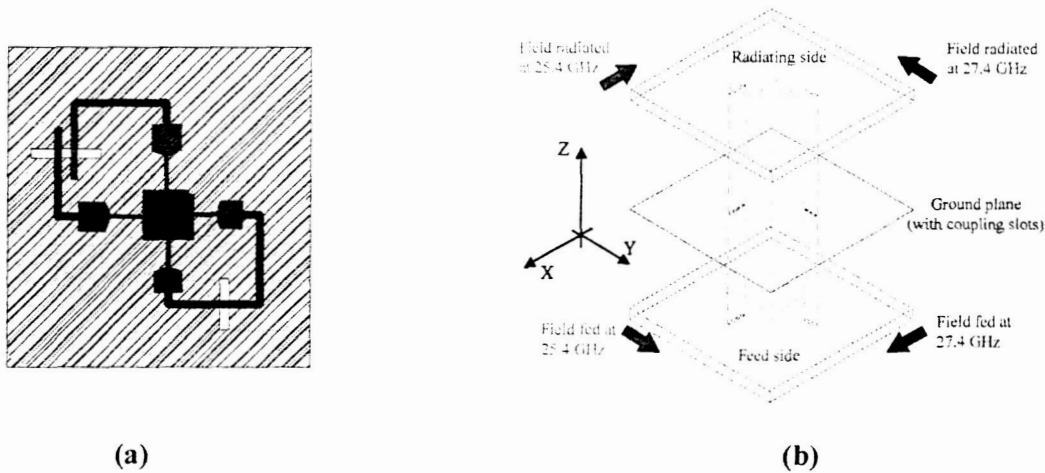


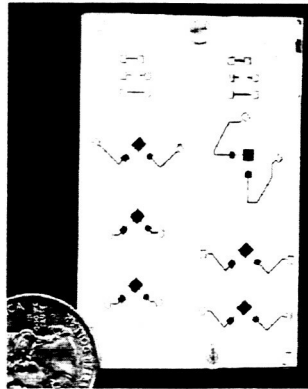
Figure 2. Layout of the unit cell of the multibeam lens array (a) and (b) view of the multilayer structure. The patch antenna has feeds at two frequencies at two polarizations. Slot couplers in the ground plane provide signal paths at both frequencies.

II. ACCOMPLISHMENTS

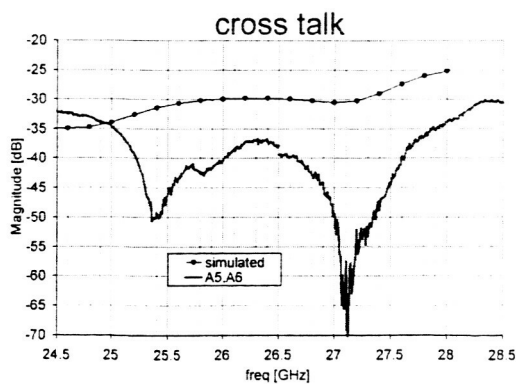
II.1. Multibeam array design – First prototype

Unit cell design

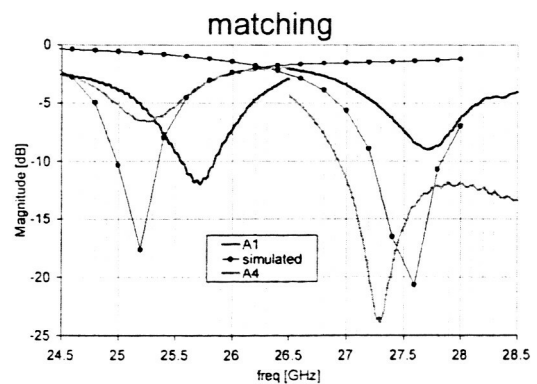
The unit cell, a sketch of which is shown in Fig.2, contains a dual-polarized dual-frequency patch antenna operating at 25.5 and 27.5 GHz. Matching circuits are designed for each feed, and slot couplers are used between the feed and radiating sides. The patch antennas and feed lines were fabricated in a separate test circuit, Fig.3a, which was tested using a probe station with results as shown in Fig.3b-c. *The measurements indicate that the antenna elements are properly matched and that the cross-talk between the two polarizations is below 30dB at both up and down-link frequencies. This measurement successfully finalized the unit array element design.*



(a)



(b)



(c)

Fig.3. (a) Photograph of test structure used to validate antenna design. (b) Measured and simulated cross-talk between the uplink and down-link feeds. (c) Measured matching at the two feeds, along with simulations.

Lens (beam) design

The design of the array and built-in multibeam network involves several degrees of freedom. We chose for the first iteration a one-degree of freedom lens, for a single focal point on the optical axis. This was chosen for simplicity and to validate fundamental operation in a relatively short time frame, knowing ahead that it was suboptimal. The parameters critical to the design are: position of antenna elements on the radiating side and length of transmission lines that enable true-time delay and determine the focal length (i.e. total volume of system). The radiating element spacing was chosen to be about 0.75λ in the horizontal and λ in the vertical dimension. Details of the design are available on request. The delay line lengths varied from 0.7λ to 1.3λ at 25.5GHz and from 0.8λ to 1.3λ at 27.5GHz across the entire array (the longest being that of the center element, and the shortest at the periphery of the array).

The substrate was chosen to be a Rogers TMM6 with a relative dielectric constant of 6 and of thickness 15mil (0.38mm). This choice is a compromise between a high-permittivity substrate that would allow for tighter array packing, and a lower permittivity that is more convenient for matching circuit design, fabrication tolerances and antenna bandwidth. Two such substrates are electrically connected with a common ground plane in a multilayer array. The signal path contains a slot coupler per element for each frequency, etched in the common ground plane.

II.2. Measurement results on first prototype

A photograph of three layers of the layers of the array (radiating side, feed side and slotted ground plane) is shown in Fig.4.

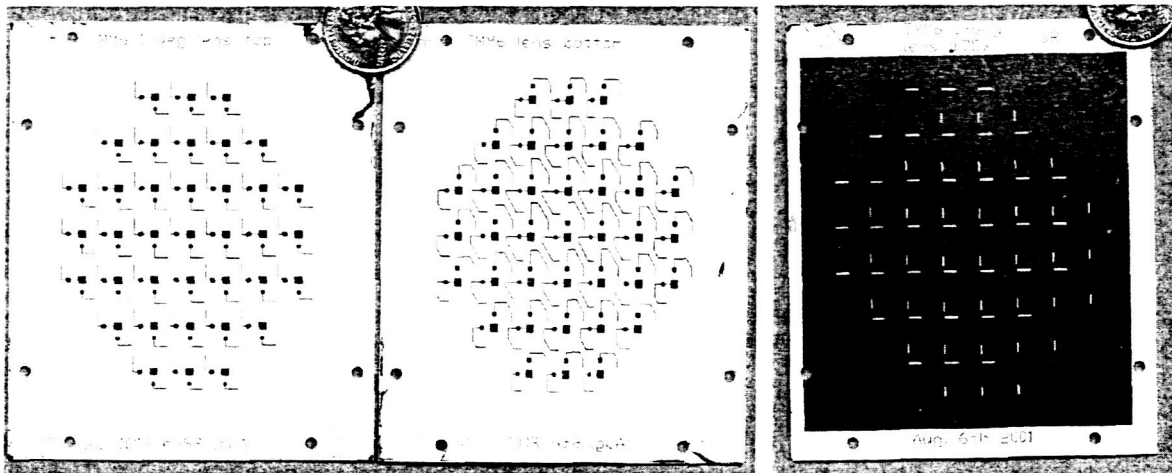


Fig.4. (a) Photograph of radiating and feed sides of the lens compared to a US\$0.25. (c) Photograph of common ground plane with slot couplers at the up and down-link frequencies.

The measured multi-beam (5 beams) radiation pattern with three open waveguide feeds positioned at 0, 15 and 30 degrees off the optical axis are shown in Fig.5 for the lower frequency, with a cross-polarization level of around -20dB . The higher-frequency beam patterns look very similar and are therefore omitted in this report.

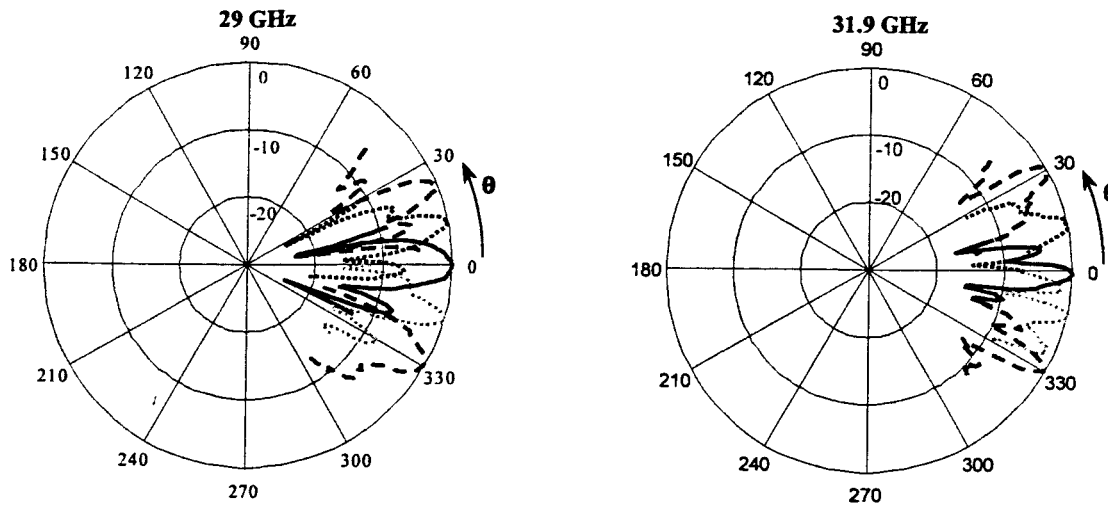


Fig.5. Measured multibeam radiation patterns in the E-plane for feeds at -30 , -15 , 0 , 15 , and 30 degrees off axis. The H-plane measurements look very similar and are omitted here.

Both operation frequencies were shifted by 7% w.r.t. the design frequency, as shown on the transfer function measurement in Fig.6. It was found that in this first prototype there was over-etching during photolithography that resulted in slightly reduced antenna dimensions, resulting in increase in resonant frequency. Since the etching was isotropic, both up and down-link frequencies were increased by approximately the same amount.

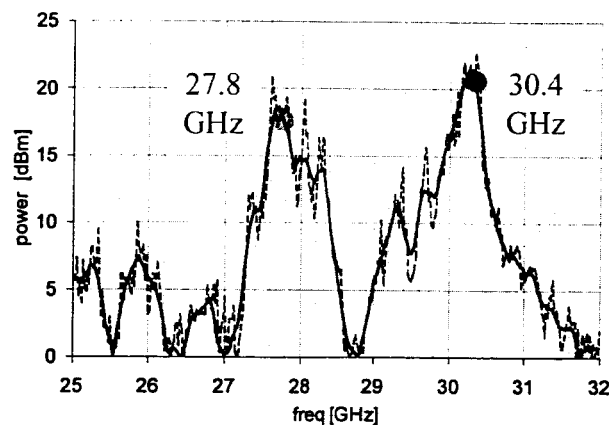


Fig.6. Measured frequency through-response of the lens indicating a shift in up and down link frequencies as compared to the designed frequencies. The shift in the lower frequency is 2.3GHz (about 7%) and in the higher it is 2.9GHz (also about 7%). The shifts are due to over-etching during the fabrication process.

It is concluded from the multibeam patterns, low beam crosstalk, low cross-polarization levels, beam shape, sidelobe levels, etc. that the first prototype successfully proved the viability of the proposed architecture, and that therefore there is merit in performing a new improved design.

II.3. Multibeam array design – Final prototype

The next design is chosen to be a lens with two degrees of freedom for a cone of best focus of ± 30 degrees. The antenna elements are rectangular patch antennas fed from the radiating edges for crossed polarization at 24.7 and 26.7GHz. The simultaneous radiation of two different frequencies requires a two-section quarter-wave transformer between the radiating edges of the patch and each of the 50-ohm feed lines, as shown in Fig.7a. The element bandwidth is measured to be 3% for both frequencies. To satisfy the beam requirement of a 10-degree half-power beamwidth, 64 elements on triangular lattice with 0.6λ and λ in the horizontal and vertical directions, respectively. Fig.7b shows the cross-section of each unit element of the DLA. The patch pair is connected with slot couplers in the antenna ground planes to a common buried delay-line sptripline layer. The delay line lengths range from 0.11λ to 1.05λ with the longest corresponding to the central array element.

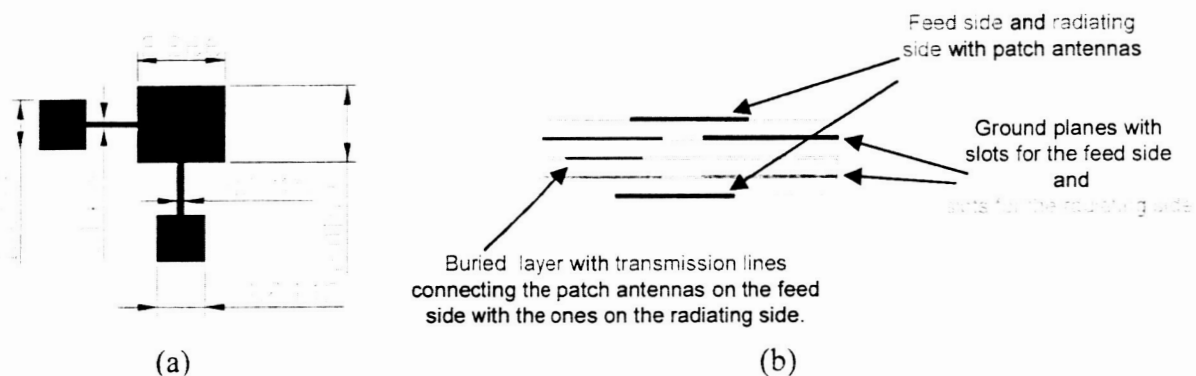


Fig.7. (a) Dual-frequency dual-polarized patch element layout, showing the two-section quarter-wave transformer between the radiating edges and the 50-ohm feed lines (not shown); (b) Sketch of the cross-section of the 5-layer lens unit cell. Notice the buried layer with the delay lines coupled to the antenna elements through resonant slots in the ground planes.

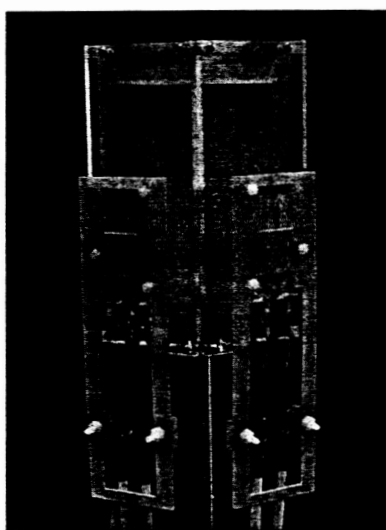


Fig.8. Photograph of packaged lens array prototype with 4 SMA connectors, one for each of the beams. Two beams are vertically polarized at the up-link frequency, and two are horizontally polarized at the down-link frequency.

The photograph of a 4-beam (2 for up-link, 2 for down-link) lens with feeds that was delivered to NASA GRC is shown in Fig.8. The photograph of the layers of the fabricated lens is shown in Fig.9, taken prior to lens assembly. All substrates are TMM6 Rogers substrates with a permittivity of 6 and a thickness of 0.38mm.

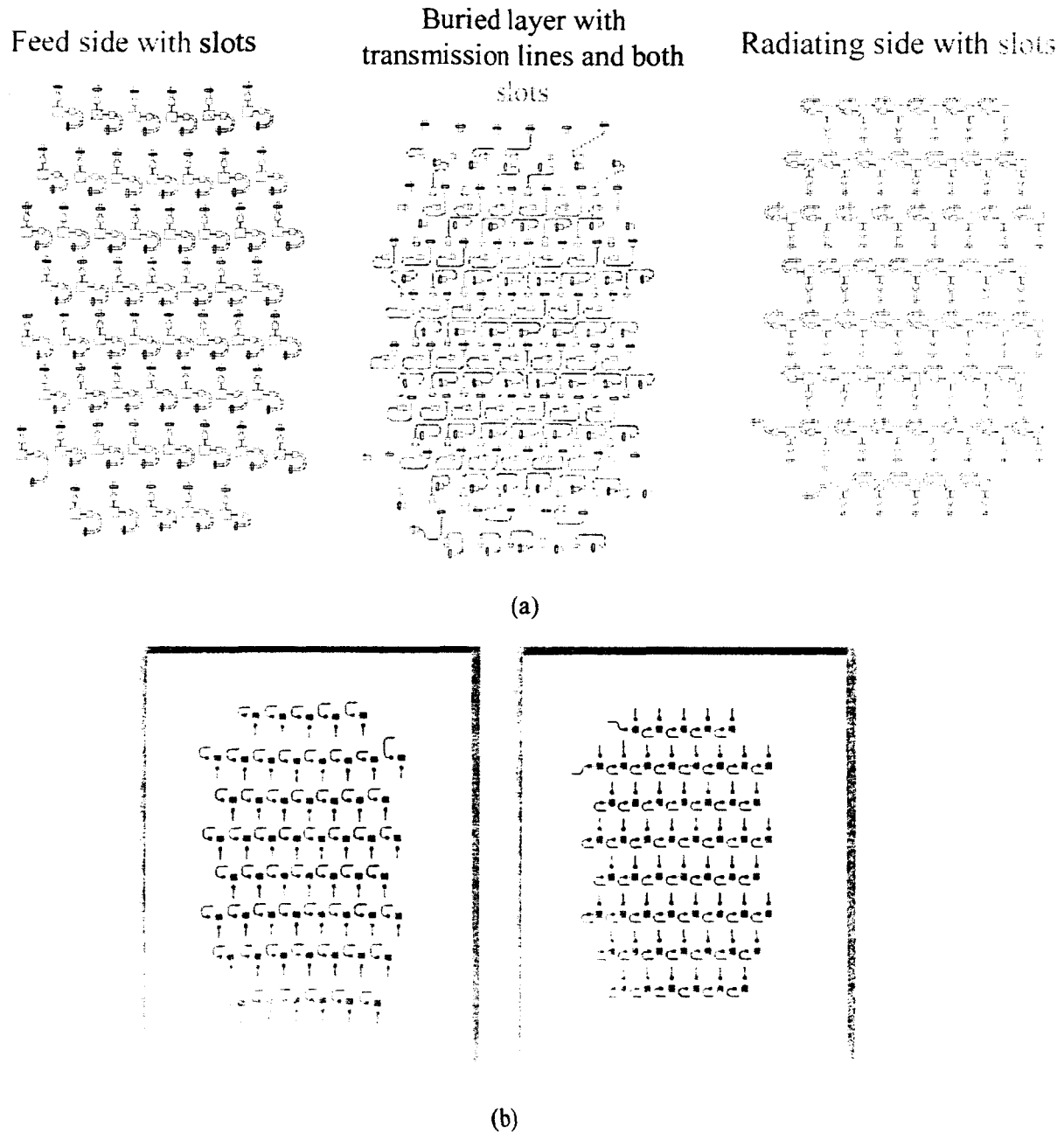


Fig.9. (a) Layout of the different layers of the 5-layer lens array: feed side, buried strip-line delay-line layer, and radiating side. (b) Photographs of the feed (left) and non-feed (right) sides of the DLA. The dimensions of the lens are 120mm (vertical) and 96mm (horizontal).

II.4. Multibeam array design – Final prototype characterization

The antenna array radiation patterns have been measured in a computer-controlled anechoic chamber at the Univ. of Colorado at Boulder and at the NASA Glenn Research Center (GRC), for both the up-link and down-link frequencies. In Fig.10 are shown the radiation patterns measured at 24.7GHz at University of Colorado for five different positions of a waveguide feed along the focal arc. The measurements performed at the NASA GRC were part of a characterization of the prototype complete with the custom designed feeds used to implement the amplitude-controlled beam steering. Each of the feeds is placed at an angle of $\pm 30^\circ$ off boresite on the DLA focal arc. The radiation patterns measured at NASA GRC at 26.7GHz for two dual-polarized dual-patch antenna feeds are shown in Fig.11. These measurements were performed to verify the measurements at the Univ. of Colorado lab.

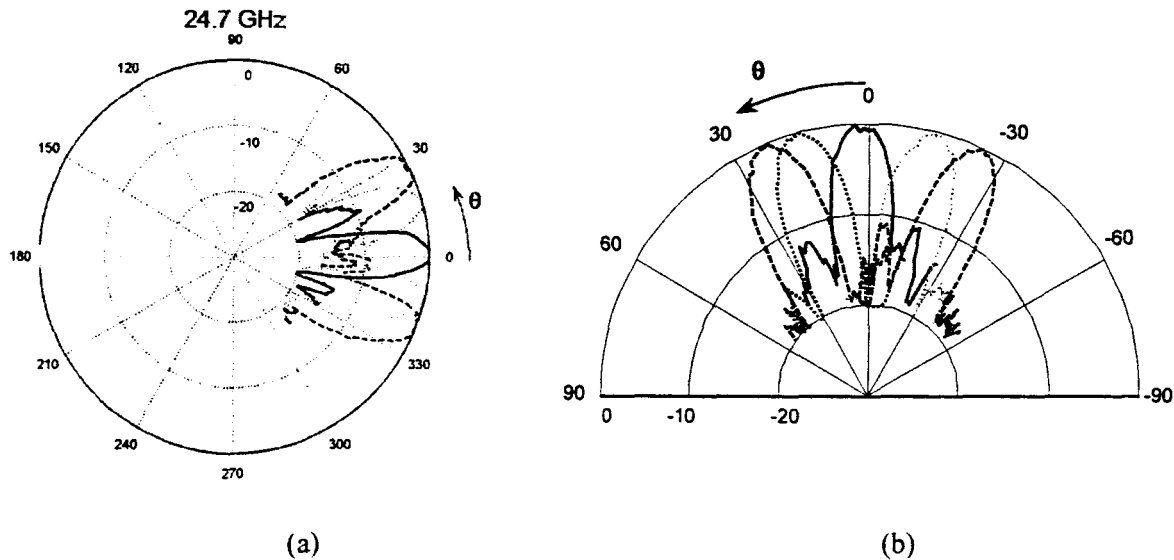


Fig.10. Measured multibeam radiation patterns at 24.7GHz (a) and 26.7GHz (b) with a waveguide feed placed at 5 different positions along the focal arc. The measurements were performed in the anechoic chamber at University of Colorado.

As part of the characterization performed at NASA GRC, the frequency response for both polarizations has been measured. In Fig.12 is shown the upper-frequency response for both feeds placed at $\pm 30^\circ$ on the lens focal arc. We believe the 2-% error in design frequency is due to fabrication tolerances (this lens was sent to a pc-board house, since our facilities are not sufficiently good for a 5-layer board assembly process).

Fig.13 shows theoretical versus measured patterns for a feed positioned at 0 and -30 degrees, where the measurements were performed at the University of Colorado at Boulder.

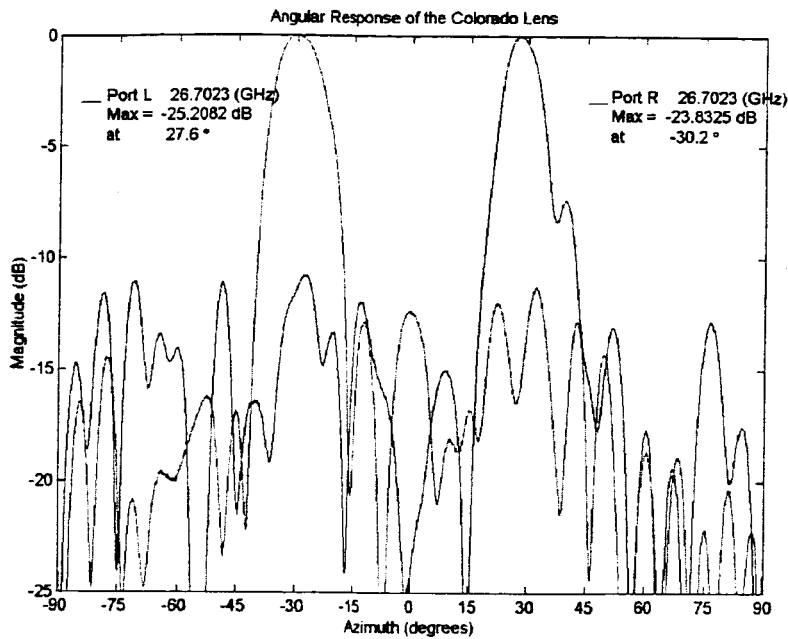


Fig.11. Measured dual-beam pattern for the 26.7GHz frequency of operation. The two lines correspond to power received at two dual-polarized patch antenna feeds for the same polarization placed at $\pm 30^\circ$ on the DLA focal arc. This measurement was performed at NASA GRC.

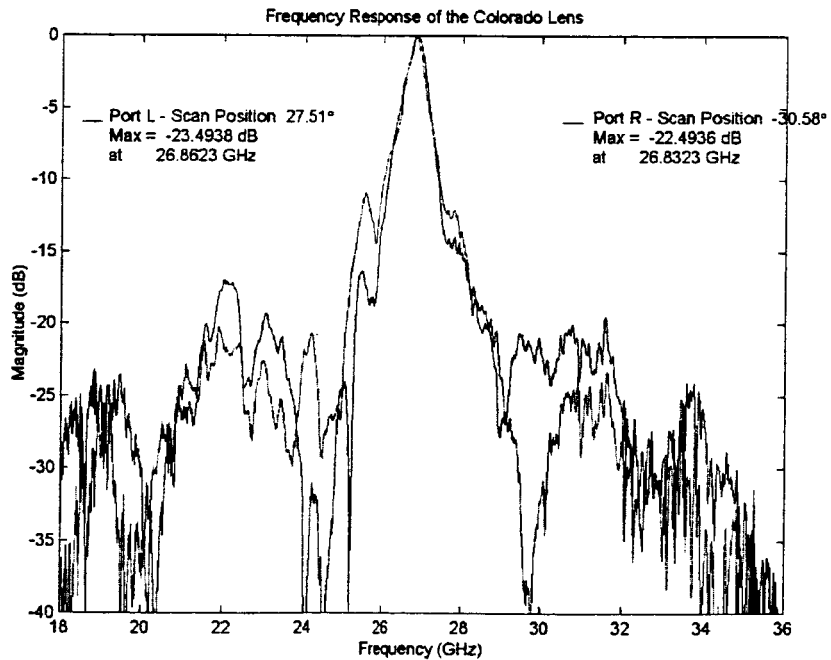


Fig.12. Measured frequency response for the upper frequency (26.7GHz): the two lines correspond to each of the two feeds placed at $\pm 30^\circ$ on the DLA focal arc. This measurement was performed at NASA GRC.

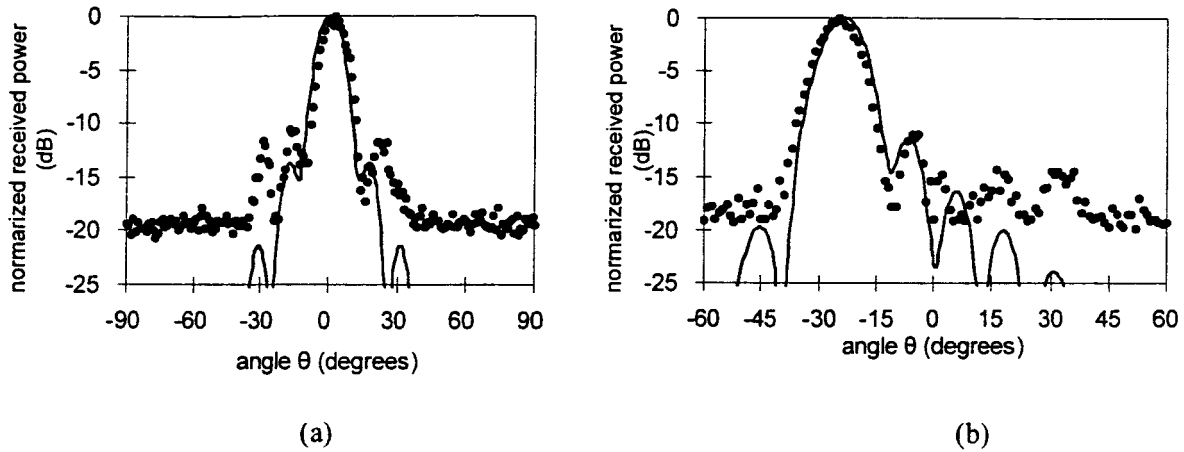


Fig.13. The measured versus calculated beam patterns for a feed positioned at 0 (a) and -30 degrees (b).

The lens array is a multibeam array with a single spatial feed, and an important parameter is isolation between the beams. In the real application, the “crosstalk” between the beams will result in power loss and unwanted coupling. In a multibeam system, the crosstalk will determine how many independent beams can be reasonably used for an N-element DLA. Theoretically, an N-element lens has N independent beams, but in practice this number will be limited by the coupling between the beams and the scan angle. Fig.14 shows measured coupling between two feed antennas positioned for -30 degree and $+30$ degree beams, along with coupling of the two feeds on the same dual frequency feed antenna of the Ka-band DLA.

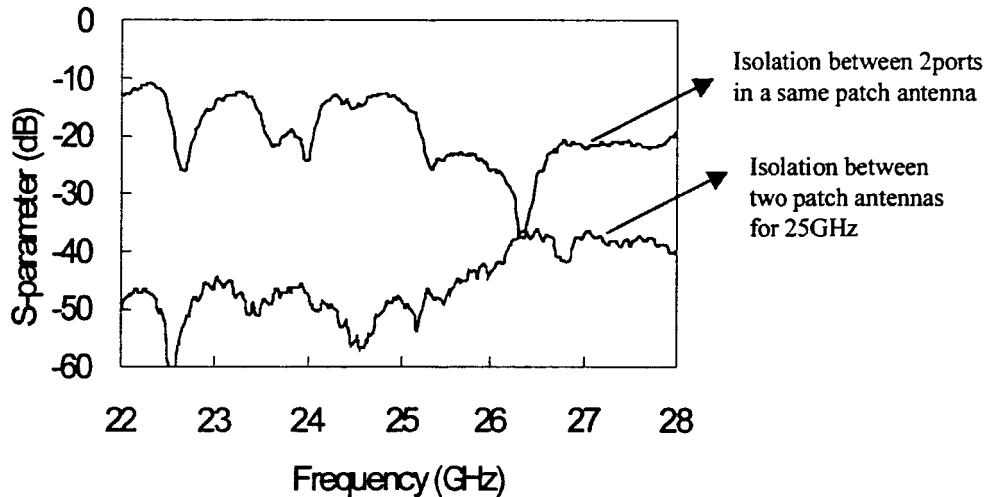


Fig.14. Measured isolation (s_{21}) between two ports on the same antenna and two ports on the two different feed antennas for the Ka-band dual-frequency DLA with feed antennas positioned at -30 degrees and $+30$ degrees off broadside.

The lens array pattern measurements are not straightforward, and it is useful to show how the measurements were performed, as illustrated in Fig.15.

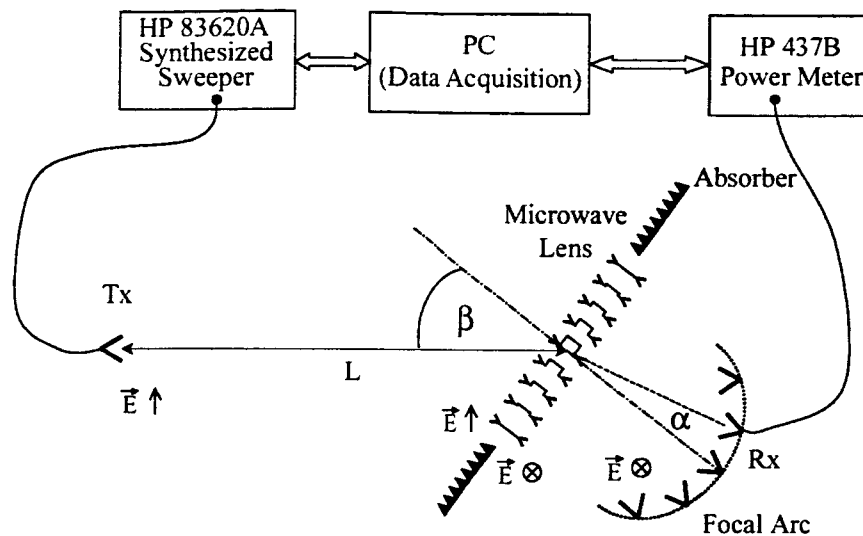


Fig.15. The lens was characterized in an anechoic chamber using the setup shown here. A standard gain horn antenna co-polarized with the non-feed side of the lens array and used as a transmitter in the measurements. For measuring radiation patterns corresponding to different beams of the multibeam lens, the lens is rotated and power detected at one receiver at a time. Linearly polarized horn antennas are used as the receiver antennas, but the same patches as the array elements can be alternatively used.

II.5. Fine beam steering using amplitude control

The final item in the statement of work was to investigate a means for fine continuous beam positioning of each of the multiple beams independently.

In our architecture, fine beam steering can be accomplished with amplitude, not phase control. Namely, if a 2-element array feed is used instead of a single feed for a given beam, amplitude variations at the feed correspond to phase steering of the radiated beam. This is due to the fact that the lens array performs a discrete spatial Fourier transform, and therefore phase steering on the image plane does not correspond to phase steering of the far-field object. However, amplitude changes in a certain spatial domain on the image (focal) plane will produce steering of the main beam in the far field. This is described in Fig.16, and simulations for a two-element patch feed are shown in Fig.17.

From the simulations for the lens with the same architecture as our prototype, it can be seen in Fig.17 that with a 20-dB power variation in the two feeds, the beam can be steered continuously by a quarter of a beamwidth on each side (a total of half of a beamwidth). The additional hardware only involves one feed antenna and a variable gain amplifier for each of the multiple beams.

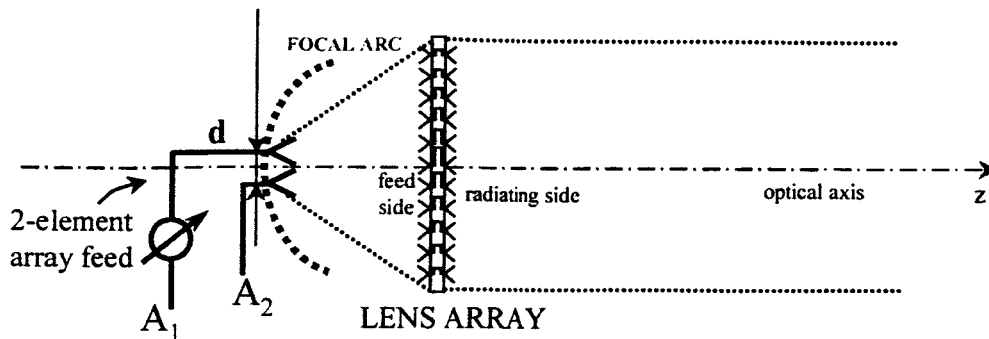


Fig.16. Schematic of setup for fine beam steering using amplitude control on multiple feeds (in this case, only two feed antennas with a single variable gain element are shown).

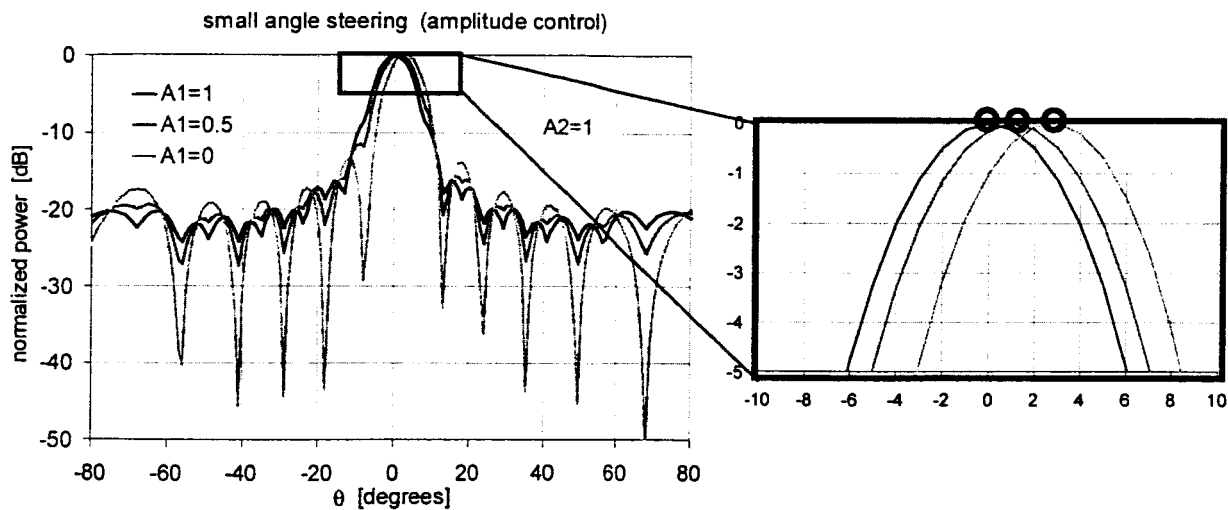


Fig.17. Simulated radiation pattern with amplitude fine-beam tuning (top). For continuous amplitude ratios of 20dB, the main beam steers continuously over half of a beam-width (bottom).

It is important (and interesting) to see the effect of feed design on output radiation pattern. Fig.18 shows simulations of the radiated lens far-field radiation pattern for a 4-element patch array feed and a 2-element array feed. Even though the 4-element array has a narrower beam-width when not used as a lens feed, it results in broadening of the lens beamwidth when placed at the focal surface. Therefore, the two-element feed is chosen for implementation for the small-angle continuous beam steering.

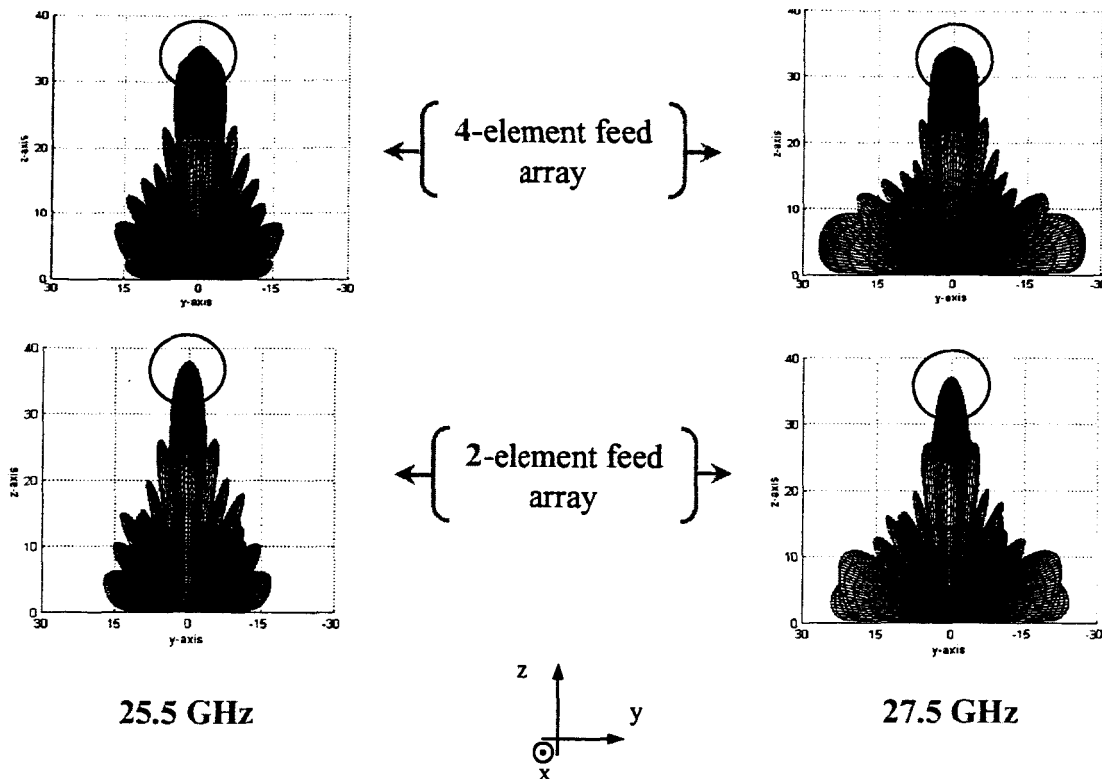
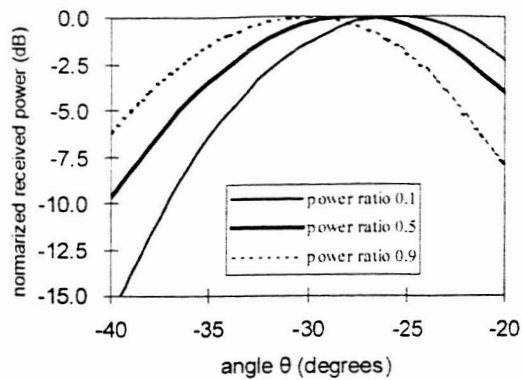
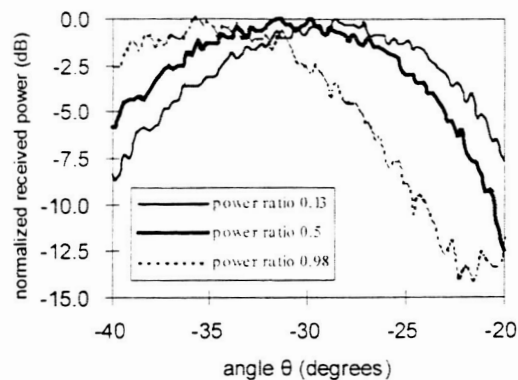


Fig.18. Simulated radiation patterns for a 4-patch antenna element array feed in E and H planes (top left and right) and for a 2-element array feed. Based on these simulations, the two-element feed was chosen for implementing small-angle continuous amplitude-controlled beam steering.

In order to demonstrate this principle, each feed of the dual-beam array was implemented with a 2-element array of patch antennas which are the same as the dual-polarized patches in the array and are spaced λ apart. The power radiated/received by each element is controlled with variable-gain attenuators or amplifiers so that the ratio between them can be varied to steer the beam. The measured and simulated small-angle steering of the beam around its fixed position at +30 degrees, are shown in Fig.19. The calculations were performed in Matlab, taking into account the lens configuration, positions of the feeds and simulated radiation patterns for the antenna elements. The boundaries for small-angle steering are set by the angular positions of the 2 elements of the feed, but depend also on the half-power beamwidth of the DLA. The measured continuous beam steering for the up and down link is shown in Fig.20a, with the red dashed line indicating what we would expect from a perfectly symmetrical lens with a perfect control at the feed. While the power at one of the two elements of the feed array is kept constant, the other is varied from a ratio of 0.1 to 1. The photograph of the circuit side of the feed array is shown in Fig.20b.

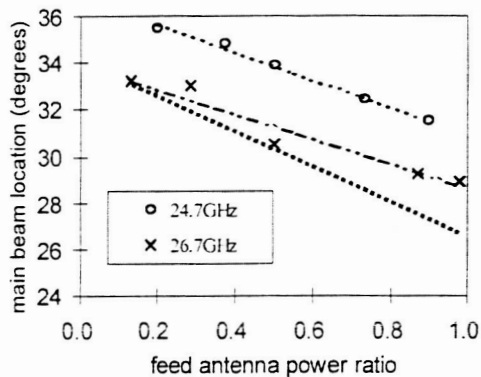


(a)

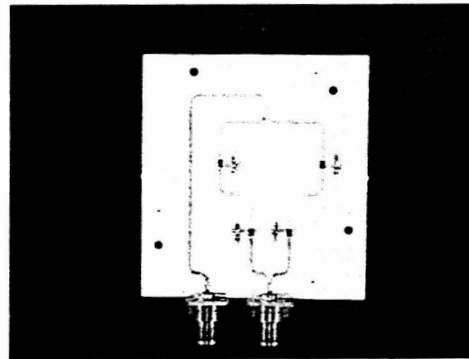


(b)

Fig.19. Calculated (top) and measured (bottom) radiation patterns of a fine-steered beam pointing at +30 degrees off optical axis, corresponding to a power ratio of 0.13 to 0.98.



(a)



(b)

Fig.20. (a) Measured amplitude-controlled beam steering versus power ratio for the two elements of the feed. The red dashed line represents symmetric ± 3 -degree beam steering around 30 degrees. (b) Photograph of circuit-side of the two-element feed for amplitude-controlled beam steering. The front side antennas are two dual-polarized patches identical to the ones comprising the lens, and spaced one wavelength apart.

In conclusion, the fine beam-steering in this new architecture is accomplished efficiently with amplitude variations on the feed side of the array. It is straightforward to independently steer each of the multiple beams.

II. 6. Comparison study with traditional phased array antennas for multibeam applications

An important issue when investigating a new architecture is comparisons with existing established methods of accomplishing the same task. In this case, the alternative approach is a phased array antenna with a separate feed network associated with each beam, and with multiple phase shifters in each feed network for fine beam steering. The comparison is summarized in

Table 1 below, with the green font indicating advantages of the given approach, and black indicating disadvantages w.r.t. the alternative approach.

The global conclusion is that for the given set of specifications, our approach with DLAs presents multiple advantages over a phased array approach to multibeam arrays with continuous fine beam tuning of each beam.

| | Phased Array (PHA) | Discrete Lens Array (DLA) |
|---|---|--|
| Radiation pattern ▪ Coupling to feed network | Potentially large | Minimal |
| Bandwidth ▪ Feeds ▪ Steering mechanism | Depend on feed implementation Phase shifters | Large: delay lines and spatial feed Large: true-time delay steering |
| Scanning properties ▪ Multibeam ▪ Fine beam steering ▪ Scan angle limit ▪ Squint | Complex and not flexible Control lines integrated with feed network. Not flexible. Limited by grating lobes Frequency-dependent feed network. | Built-in, flexible Control lines completely separated from spatial feed. Partial flexibility. Grating lobes and extra feed loss for large scan angles. True time delay: low (or no) squint |
| Loss | Lower losses for small arrays | Lower losses for large arrays (>50 elements) |
| Weight and volume | Possibly less volume | Less weight |
| Power consumption | Amplifiers and phase shifters | Only amplifiers |
| Reliability | Requires redundancy | Graceful degradation |
| Cost | Phase shifters, weight, reliability, design inflexibility | Lighter weight, inherent reliability, design flexibility |

Table 1. Comparison between a multibeam phased array and a multibeam lens array.

III. CONCLUSION

In summary, this report presents results that confirm the originally proposed approach to multibeam arrays for satellite applications. All the items from the statement of work have successfully been completed and were detailed in monthly reports. Only the main and final results are given in this report for clarity.

The presented results show that the next logical steps in the implementation of these multibeam arrays are:

- improving the packaging
- adding gain in receive and transmit
- investigating the limitations on the number of usable beams, etc.

We hope to have an opportunity in the future to work in this area.

Recognition and Awards

Dr. Romisch, the research associate funded under this grant, has been nominated for the URSI Young Scientist award and in the event she is awarded it, she will be presenting this work as her accomplishment. The awardees will be announced in May 2002.

Prof. Popovic was elected a Fellow of IEEE in 2002, and received the ASEE/HP Terman Award in 2001.

Prof. Popovic was nominated for the NASA Distinguished Achievement Award, June 2003.

Publications (directly related to the work supported by NASA, or partly related to the work)

1. "Multibeam planar discrete millimeter-wave lens for fixed-formation satellites," Romisch, S., Bell, P., Popovic, D., Shino, N., Popovic, Z., *Digest of 27th URSI General Assembly, Maastricht, Amsterdam, Aug 2002. – Young Scientist Award (S. Romisch)*
2. "Multibeam Discrete Lens Arrays with Amplitude-controlled Steering," Stefania Römisch, Darko Popović, Naoyuki Shino[§], Richard Lee*, Zoya Popović, *IEEE MTT International Microwave Symposium Digest*, Philadelphia, June 2003.
3. "Multibeam Phased Array Antennas," R.Q. Lee, S. Romisch, Z. Popovic, *presented at the 2002 Antenna Applications Symposium*, Allerton, September 2002.

Related papers:

"Spatial Processing with Lens Antenna Arrays for Direction-of-Arrival Estimation," Do-Hong, Tuan; Hagerty, Joseph A.; Popovic, Zoya; Russer, Peter: *Digest of 27th General Assembly of the International Union of Radio Science* (2002) Aug.

"Active and Smart Antenna Arrays," *Invited plenary talk at the Annual Meeting of the Argentine Physical Association, Cordoba, Argentina, Sept 2002*

"Multibeam Spatially-Fed Antenna Arrays," Sebastien Rondineau, Stefania Romisch, Darko Popovic, Zoya Popovic, *invited talk, 2003 IEEE Topical Conference on Wireless Communication Technology*, to be held in Hawaii, October 2003.

Theory on lenses is described additionally in:

"Multibeam antennas with polarization and angle diversity," D. Popovic, Z. Popovic, *IEEE Trans. Antennas and Propagation, Special Issue on Wireless Communications*, pp. 651-657, May 2002.

Submission:

A journal paper entitled "Multibeam mm-wave lens array with amplitude-controlled fine beam-steering," by Stefania Romisch, Naoyuki Shino, Darko Popovic, Patrick Bell and Zoya Popovic, is currently under preparation for submission to the IEEE MTT Transactions.